Low-Loss Micromachined Filters for Millimeter-Wave Communication Systems

Pierre Blondy, Andrew R. Brown, *Student Member, IEEE*, Dominique Cros, and Gabriel M. Rebeiz, *Fellow, IEEE*

***Abstract*— High-performance planar micromachined filters at 37 and 60 GHz are presented. The filters consist of a 3.5% bandwidth two-pole Chebyshev filter with transmission zeros at 37 GHz, 2.7% and 4.3% bandwidth four- and five-pole Chebyshev filters at 60 GHz, and an 8% bandwidth elliptic filter at 60 GHz. Silicon micromachining techniques combined with micropackaging have been applied to allow for very high-Q resonators resulting in low-loss filters. The 37-GHz two-pole filter exhibits a 2.3-dB port-to-port insertion loss. The 2.7% and 4.3% four- and five-pole Chebyshev filters at 60 GHz exhibit 2.8- and 3.4-dB insertion loss, and the 8% elliptic filter exhibits a 1.5-dB insertion loss. These values show a large reduction of insertion loss compared to conventional planar techniques, and can be used for planar low-cost millimeter-wave wireless communication systems.**

***Index Terms*— Micromachining, millimeter wave, packaging techniques, planar filters.**

I. Introduction

MILLIMETER-WAVE communication systems are expanding rapidly as they offer many advantages over conventional wireless links. They allow the use of very wide-band radio links suitable for inter satellite communications and personal communications.

We have focused on 38-GHz radio links for base station communications in PCS networks and upcoming 60 GHz multipurpose telecommunication systems [1], [2]. Waveguide components are widely used at these frequencies and offer very good performance. However, they result in high production costs and bulky systems. Planar circuits are not currently being used for this application because the level of required performance cannot be reached by using conventional methods. Conventional planar structures suffer from radiation from the resonators into the substrate and from high resonator ohmic loss. This results in low resonator Q giving high insertion loss and poor filter rejection. Micromaching techniques have been shown to enhance filter performance by reducing the radiation, ohmic, and dielectric losses of resonators. The micromachining technique consists of removing the dielectric material up to a thin membrane that suspends the planar filters. Also, the filters are packaged in a micromachined cavity. The combination of bulk micromachining by removal of the substrate and self packaging reduces radiation loss both into air and dielectric substrate modes, and also greatly reduces ohmic loss by allowing for very wide microstrip lines. In the past, micromachining techniques have been successfully applied to K- and W-Band microstrip membrane supported filters [3], [4]. In this paper, we report the design, fabrication, and measurements of several new planar, micropackaged bandpass filters.

Transmission zeros are highly desirable in many applications to achieve a sharp out of band rejection with a reduced number of poles compared to conventional Chebyshev functions. Therefore, we have investigated two- and four-pole filters with transmission zeros. The four-pole design has a moderate bandwidth (8%) and can be used as a preselector filter. A narrow-band filter has been fabricated using conventional Chebyshev response functions, and can be used as diplexing units in communication systems. Moreover, it is important to note that the membrane filters can be easily combined with active devices (low noise amplifiers, power amplifiers) and high efficiency planar antennas. This will result in very low-loss integrated front-ends for millimeter-wave applications.

II. Fabrication

A stress compensated 1.4-μm membrane layer consisting of SiO_2–Si_3N_4–SiO_2 is deposited on a high resistivity 525-μm-thick silicon substrate using thermal oxidation and low-pressure chemical vapor deposition. After the membrane is deposited, the circuit is patterned on the top side of the wafer using either standard 2.5-μm gold electroplating technique, for 37-GHz filter, or 1-μm evaporated gold and liftoff procedure for the 60-GHz filters. Next, the silicon is completely etched under the filter circuit until the filter is left standing on the thin dielectric membrane. At the same time, via grooves are opened all around the filter circuit in order to ensure a complete shielding of the structure. The lower cavity is etched in a 525-μm low-resistivity wafer and metalized with gold. The upper cavity is formed by double-side etching. First, a selective etch is performed on the upper side of the wafer to begin probe window openings. Next, the lower side is patterned and the wafer is etched on both sides to open the probe windows and to form the upper cavity ground plane. The upper cavity is also metalized with gold. The three wafers are stacked together and

Manuscript received March 30, 1998; revised August 29, 1998. This work was supported by the Army Research Office under the MURI Program under Contract DAAH04-96-1-0001.

P. Blondy and D. Cros are with IRCOM, University of Limoges, 87060 Limoges Cedex, France.

A. R. Brown and G. M. Rebeiz are with the Radiation Laboratory, Department of Electrical Engineering, University of Michigan, Ann Arbor, MI, 48109 USA.

Publisher Item Identifier S 0018-9480(98)09206-0.

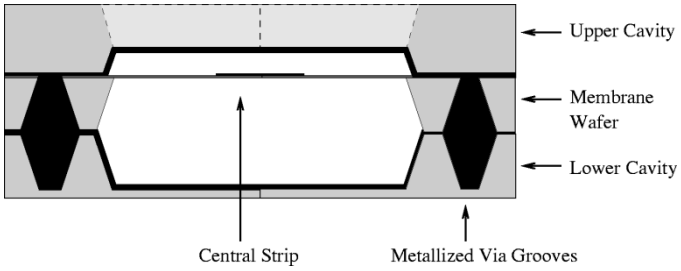

Fig. 1. Transverse section of the microstrip structure.

silver epoxied to form a completely shielded, self packaged circuit, as shown in Fig. 1.

For all the filters presented hereafter, the operating mode is microstrip with wide transverse dimensions.

III. Design Procedure

The design procedure for all filters was done in a similar manner to coupled cavity filter design. As it was pointed out in [5], this technique [6]–[8] is very general and can be virtually applied to any type of filter with narrow or moderate bandwidth. Since the filters presented are symmetric, only the first half of the filter will be discussed. A low-pass prototype filter is first chosen giving the values of g_i. The external Q of the first and last resonator is then set. The ideal external Q of the filter is found from

$$Q_{\text{ext}} = \frac{f_0}{\Delta f} g_0 g_1 \tag{1}$$

where f_0 is the center frequency of the filter and Δf is the bandwidth of the filter. The external Q of the filter is related to loading effect from coupling the first resonator to the input feed line. With the resonator coupled, the value of Q_{ext} can be found from taking the fractional bandwidth defined as the bandwidth over a 180° phase shift in S_{11} around the resonant point of the coupled resonator [Fig. 2(a)]. If the 180° bandwidth is defined as Δf_{01}, then the Q_{ext} is simply

$$Q_{\text{ext}} = \frac{\Delta f_{01}}{f_0}. \tag{2}$$

By varying the coupling from the input line to the first resonator to alter Q_{ext}, the coupling can be optimized to match the ideal Q_{ext} derived from the low-pass prototype filter.

Next, the inter-resonator coupling values, k_{ij}, are computed and related to the physical dimensions of the resonators. The ideal values of k_{ij} are derived from the low-pass prototype from the expression:

$$k_{ij} = \frac{\Delta f}{f_0} \frac{1}{\sqrt{g_i g_j}}. \tag{3}$$

This is related to the design by the resonant frequency of the ith and jth coupled resonators for even and odd mode excitations, as shown in Fig. 2(b). For a given geometry, the k_{ij} is given by [9]

$$k_{ij} = \frac{f_{\text{even}}^2 - f_{\text{odd}}^2}{f_{\text{even}}^2 + f_{\text{odd}}^2} \tag{4}$$

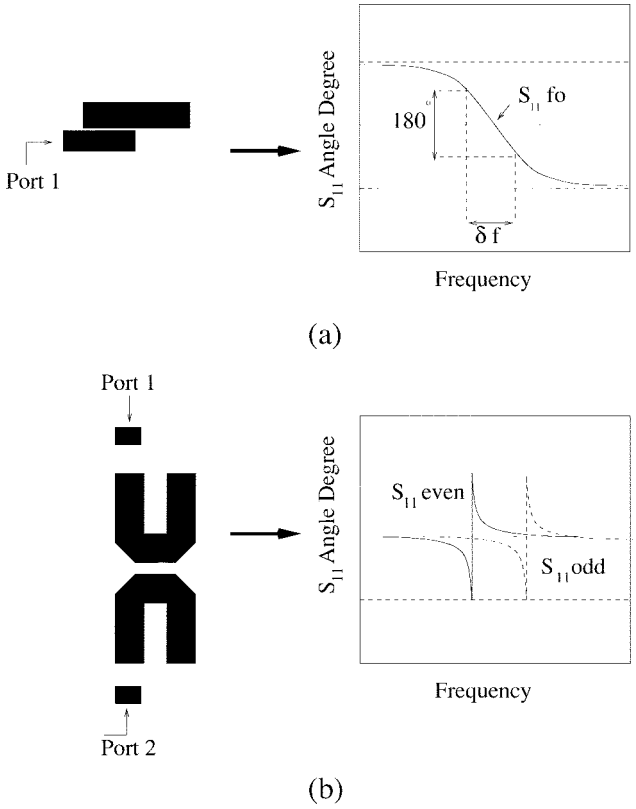

Fig. 2. Summary of the design procedure.

where f_{even} and f_{odd} are the resonant frequencies for the two coupled resonators under even- and odd-mode excitations. The coupling between the two resonators determines f_{even} and f_{odd} and is optimized so that k_{ij} is the same as that calculated by the low-pass prototype function.

The designs of the filters presented later in this paper were computed using the method of moments based HP-Momentum.[1] This is a $2\frac{1}{2}$D software tool that does not allow for the transition from silicon to membrane to be taken into account. The fabricated filters presented later in this paper were designed neglecting the transition from silicon CPW input lines to membrane supported microstrip lines. Therefore, Q_{ext} is not accurately estimated when simulated using HP-Momentum. Accurate designs should use a full 3-D simulation tool for predicting the value of Q_{ext}. Because of the silicon CPW to membrane supported microstrip discontinuity, the input structure response can only be estimated using $2\frac{1}{2}$D simulation tools.

Quasi-TM modes can be excited in the vicinity of the transition. The substrates used are relatively thick, and to ensure a single mode of propagation at the input of the filter, the cutoff frequency of the first higher order mode must be above the frequency of interest for the filter. The cutoff frequency of the first higher order mode has been calculated using a finite element based software tool [10] for several different values of substrate thickness (Fig. 3). With a 525-μm-thick wafer, the distance between vias on each side of the

[1] Momentum, Hewlett-Packard, CA.

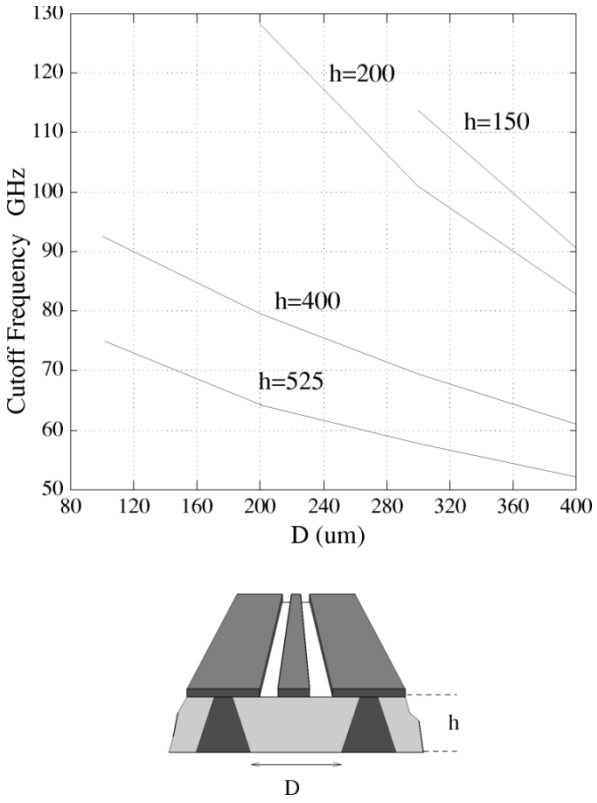

Fig. 3. Quasi-TM-mode frequency cutoff for various substrate heights. This represents the mode cutoff of the input CPW line first higher order mode.

CPW access line was set at 100 μm in order to push the first quasi-TM mode cutoff frequency to above 70 GHz.

IV. Single-Resonator Measurements

Single membrane supported resonators at 37 and 60 GHz were fabricated. At 37 GHz, the resonator is a single $\lambda_0/2$ microstrip line with a ground to conductor height of 200 μm and a line width of 700 μm. The measured unloaded Q of this resonator is 412 at 37 GHz. Two different resonators were fabricated at 60 GHz for comparison. Both resonators have a ground plane to conductor spacing of 250 μm with widths of 500 and 700 μm. The 500-μm lines had a measured unloaded Q of 454 and the 700-μm lines had a measured unloaded Q of 503.

The three structures described above were simulated using method of moments based HP-Momentum, a finite-element tool, an empirical model from Linecalc,[2] and a code based on surface impedance method called Simian [11]. For the simulations, the conductivity of the gold lines was assumed to be $3.9 \times 10\hat{}7\ \Omega^{-1} \cdot \mathrm{m}^{-1}$. The results for the simulations and measurements are summarized in Table I. The values based on Linecalc, MoM, and FEM all overestimate the value for the unloaded Q conciderably. However, Simian models the loss very accurately and is within 5% of the measured values. The measured Q_u values are 10 $\times$ larger than microstrip resonators on GaAs or Silicon, and two $\times$ larger than resonators on low dielectric constant substrates such as Teflon.

[2] Linecalc, Hewlett-Packard, CA.

TABLE I
Comparison Between Measured and Simulated Values of Unloaded Q

Unloaded Q	w=700 μm h=200 μm fo=37 GHz	w=700 μm h=250 μm fo=62 GHz	w=500 μm h=250 μm fo=62 GHz
linecalc [12]	474	665	606
FEM [11]	442	661	610
MoM [10]	470	613	536
Simian [13]	403	525	474
Measured	412	503	454

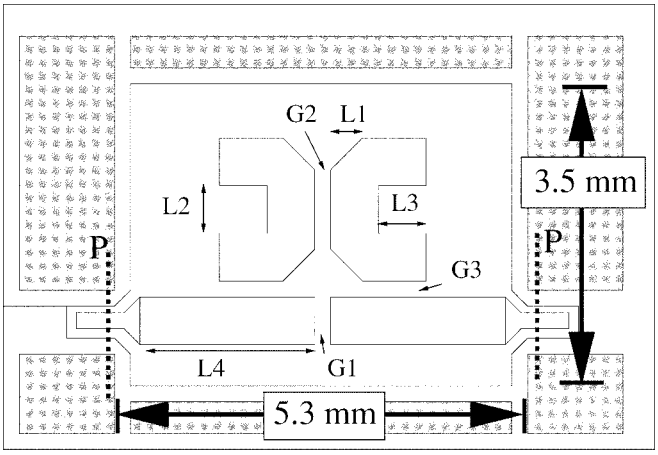

Fig. 4. Layout and dimensions of the two-pole filter at 37 GHz. L1 = 420, L2 = 470, L3 = 1280, L4 = 2400, w = 700, G1 = 75, G2 = 95, G3 = 50 (Dimensions are given in micrometers).

V. 37-GHz Two-Pole Filter

A two-pole filter was fabricated using the micromachining process described above. The input and output lines of this filter topology are capacitively coupled and the hairpin resonators are magnetically coupled. This design gives a pair of transmission zeros causing a sharper filter rolloff. The ground plane to conductor height is 200 μm with 700-μm-wide resonators of 2.5-μm electroplated gold. The design started from a Chebyshev two-pole prototype [7]. Full wave optimization was performed to adjust the gap between the feed lines for the transmission zeros while keeping the ripple in the passband as low as possible. After optimization, the Q_{ext} was found to be 39, and k_{12} is 0.028. The filter layout is shown in Fig. 4. The filter was measured using an HP8510C network analyzer. Calibration was done using a TRL procedure with NIST MULTICAL software [12], [13]. The calibration planes are taken on silicon CPW ports. The results presented include the silicon CPW to the membrane supported microstrip transition. Full wave computations obtained by HP-Momentum agree very well with measurements, although the transition has not been taken into account by these simulations. We believe that the lack of influence from the transition is due to the $\lambda/4$ feedlines that results in a magnetic field maximum at the transition plane. This reduces the effects of both the dielectric substrate and the CPW to microstrip discontinuities. The measured S_{11} rose from the simulated value of -15 dB to -12 dB. Therefore, we have modeled the transition by a series 0.04-nH inductance, added to Momentum simulations.

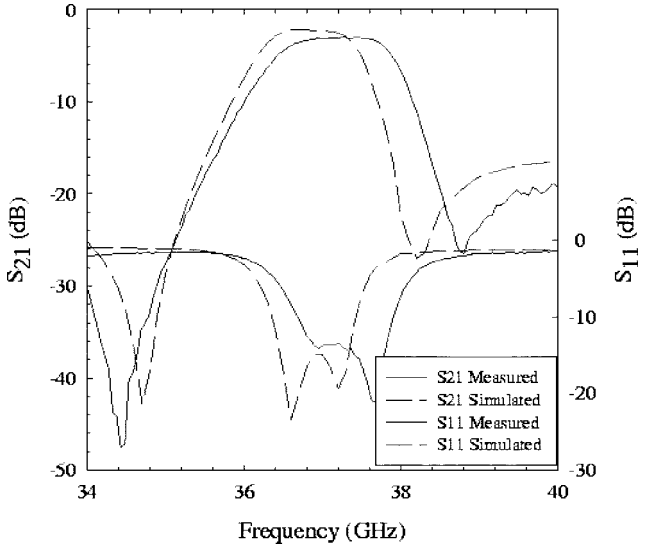

Fig. 5. Measured and simulated response of the two-pole filter at 37 GHz.

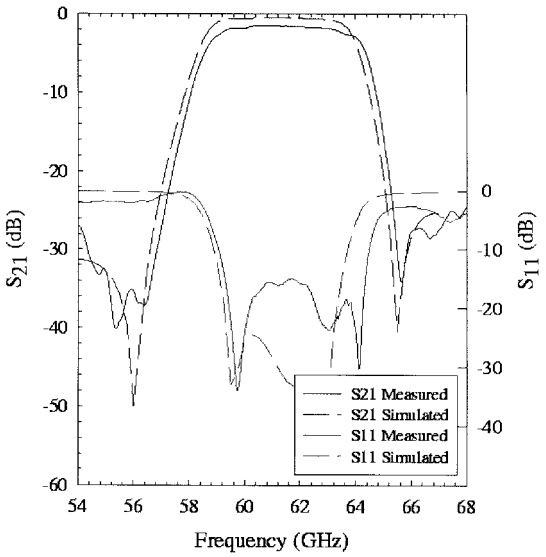

Fig. 7. Simulated and measured results for the four-pole elliptic filter.

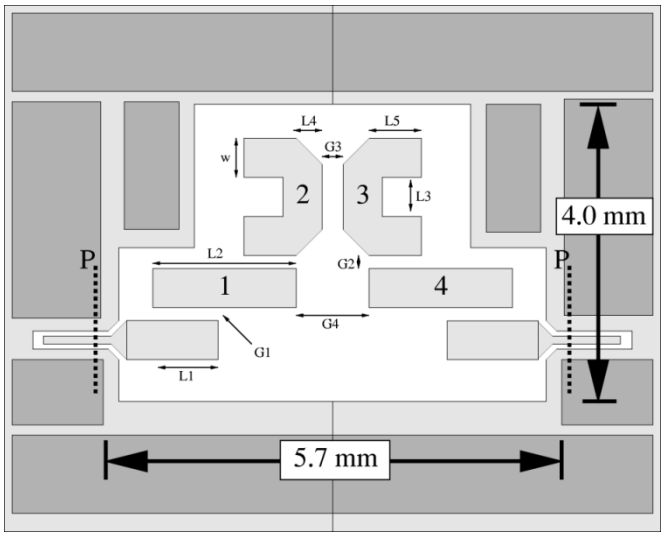

Fig. 6. Layout of the four-pole 8% filter at 61.5 GHz. L1 = 820, L2 = 2180, L3 = 645, L4 = 300, L5 = 675, w = 500, G1 = 15, G2 = 200, G3 = 175, G4 = 625 (Dimensions are given in micrometers).

This gives a good agreement between mesured and computed S_{11}, as shown in Fig. 5. This also models very well the second transmission zero behavior, that is not as sharp as it would be, if the transition was negelected in the simulations. The insertion loss increased from the theoretical insertion loss of 1.4–2.3 dB due to transition effects and a decrease in unloaded Q from the simulations to the actual measurements. The relative bandwidth is 3.5%.

VI. 60-GHz Four-Pole Elliptic Filter

A novel four-pole filter topology (Fig. 6) was developed based on the design of the two-pole filter presented above to give a true elliptic response with very low loss on a compact, planar structure. The filter topology is demonstrated for an 8% bandwidth filter centered at 61.5 GHz. The input and output are coupled to straight $\lambda/2$ resonators. The straight resonators couple to a set of bent U-shaped resonators which are magnetically coupled. The straight resonators are also capacitively coupled to each other giving the nonadjacent resonator coupling necessary for an elliptic response, [14]–[16]. In order to fabricate the bent U-shaped resonator at 60 GHz, the conductor width was decreased to 500 μm, and to still maintain a high-quality factor, the ground plane to conductor spacing was increased to 250 μm. The resonator unloaded Q is 454 from Table I. The metallization patterning was done using 1-μm evaporated gold and liftoff procedure in order to take advantage of the smooth metallization surface obtained. Shielding is made using via grooves surrounding the filter. The single resonator unloaded Q was measured to be 454 as discussed in Section IV. The filter design was done using HP-Momentum starting from a four-pole 8% bandwidth Chebyshev prototype. Cross coupling between resonators 1 and 4 was computed using the formulas given in [14] and they were adjusted to the desired response. The coupling coefficients can be extracted from full-wave simulations. Let k_{nm} be the coupling coefficient between resonator n and m (see Fig. 6). k_{12} and k_{23} and k_{14} are not independent in this design. The resonator spacing is varied to give the correct value for k_{23}. Next, the distance from the ends of resonators 1 and 4 is varied to give the correct k_{14}. Finally, the gap between resonators 1 and 2 is adjusted to give the correct k_{12}. For the 8% filter, $k_{12} = 0.072$, $k_{23} = 0.062$, $k_{14} = -0.013$, $Q_{\text{ext}} = 12$. The measured and simulated responses are presented on Fig. 7. The agreement between simulated and measured responses is very good, and the frequency shift between simulated and measured response is less than 1% of the center frequency. The relative passband is 8% and the measured port to port (including transition) insertion loss is 1.5 dB with a return loss below -14 dB. The calculated insertion loss are 0.9 dB neglecting the transition. As with the two-pole filter, the transition has little effect on the measured performance of this filter. The measured out of band rejection is better than 35 dB, and the whole filter is smaller than 4 $\times$ 6 mm^2.

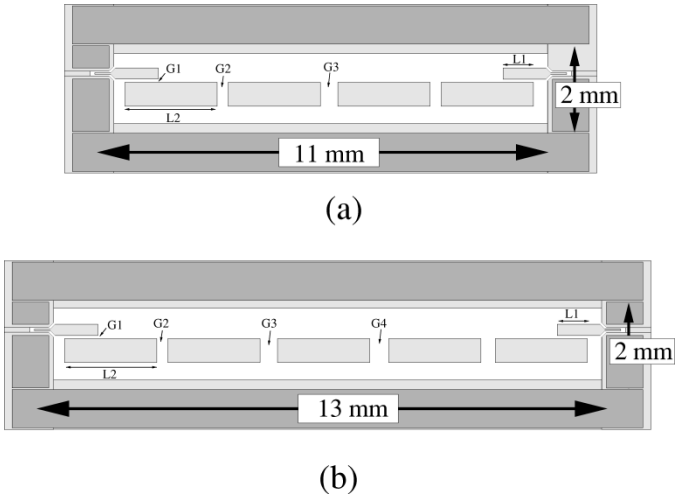

Fig. 8. Four- and five-pole filter layout. (a) L1 = 860, L2 = 2250, G1 = 55, G2 = 425, G3 = 480 − (b) L1 = 860, L2 = 2100, G1 = 55, G2 = 400, G3 = 450 (Dimensions are given in μm).

VII. 60-GHz Four- and Five-Pole Chebyshev Narrow Bandwidth Filter

Narrow-band four- and five-pole filters were fabricated using 700-μm-wide capacitively coupled half-wavelength microstrip resonators with a ground plane spacing of 200 μm (Fig. 8). The fabrication technique is the same as previously described for the 60-GHz elliptic filter. The four-pole filter prototype is a Chebyshev filter, 0.05-dB ripple, 3% relative bandwidth, centered at 59.5 GHz. The five-pole filter is based on a 4% bandwidth, 0.05-dB ripple Chebyshev function with a center frequency of 62.5 GHz. A similar method was used for computing the resonator coupling as described in the previous section except for the nonadjacent resonator coupling. As with the previous designs, this was simulated and designed with HP-Momentum neglecting the effects of the transition. The results for the four-pole filter are presented on Fig. 9. The measured CPW port to port insertion loss is 2.8 dB and the measured relative passband is 2.7%. The agreement between measured and simulated data is excellent since the frequency shift is less than 1% the center frequency and the calculated insertion loss is 1.4 dB. The return loss is better than 14 dB, including the transition from CPW to microstrip. The insertion loss is higher than the simulated insertion loss, but the simulations were done neglecting the CPW to microstrip transition. The five-pole filter results are shown in Fig. 10. The measured insertion loss is 3.4 dB with a relative pass band of 4.3%. Measured out of band rejection is better than 40 dB. The return loss is large, but that has not yet been optimized. As with the four-pole filter, the insertion loss is larger than the simulated insertion loss.

There is room for improvement in these filters, since it can be seen from the S_{11} curves presented that loss mechanism needs a close look. The transition is a 3-D problem with multimodal effects, and this part of the design needs further investigation to decrease the insertion loss and improve out of band rejection. Also, there is nothing to prevent a slot line mode in the CPW feedline at the discontinuity. Future designs should include an air bridge process. Still, we believe that the

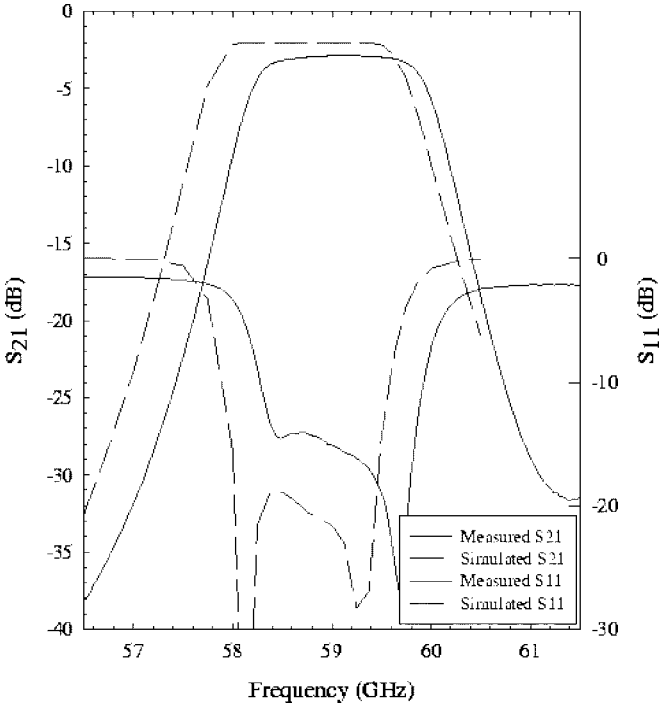

Fig. 9. Measured and Simulated response of the Chebyshev four-pole filter.

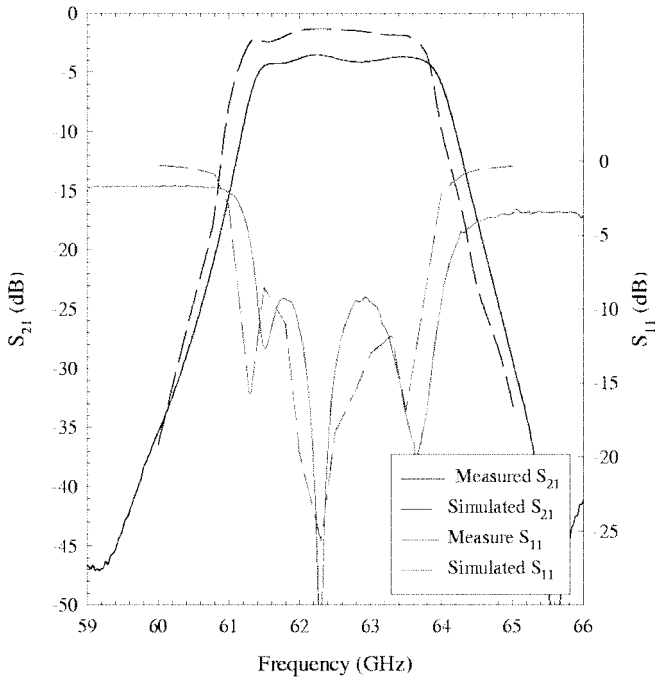

Fig. 10. Measured and Simulated response of the Chebyshev five-pole filter.

results presented are the lowest insertion loss *planar* 3 and 4% filters to date and can be integrated for use as a frequency selective diplexer.

VIII. Conclusion

In this paper, we have presented measured results obtained after conception, realization and measurement of micromachined narrow and moderate bandwidth filters. The measured insertion losses are low compared to other planar filters at

these frequencies. The design methodology used allows one to design membrane filters regardless of the transverse dimensions, and to implement several transfer functions such as pseudo-elliptic or Chebyshev. The quarter wavelength feeding structure minimizes the effect of the transition. The Q_{ext} has been estimated using MoM simulation, and this excitation configuration allowed to keep small return loss, both in experimental and simulated results. Still, this part of the design needs further improvement and testing. These circuits are very low cost, considering that they are made with MMIC fabrication techniques, and from widely available substrate. The optimization of the transverse dimensions and shielding technique will allow to further reduce the insertion loss. The combination of such filters with high efficiency planar membrane antennas and active MMIC through the CPW access will result in compact, low-loss and low-cost receiver front ends for personal wide-band telecommunication systems.

ACKNOWLEDGMENT

The authors wish to thank Dr. G. Ponchak from NASA Lewis Research Center, for providing the 60-GHz measurement setup. One of the authors, P. Blondy, wishes to thank Prof. P. Guillon, from the University of Limoges for his constant support and encouragement during this work.

REFERENCES

[1] H. H. Meinel, "Commercial applications of millimeterwaves. History, present status and future trends," *IEEE Trans. Microwave Theory Tech.*, vol. 43, pp. 1639–1653, July 1995.
[2] J. Burns, "The application of millimeter wave technology for personal communication networks in the United Kingdom and Europe: A technical and regulatory overview," in *IEEE MTT-S Symp. Dig.*, 1994, pp. 635–638.
[3] C. Y. Chi and G. M. Rebeiz, "Conductor loss limited stripline resonator and filters," *IEEE Trans. Microwave Theory Tech.*, vol. 44, pp. 626–629, Apr. 1996.
[4] S. V. Robertson, L. P. B. Katehi, and G. M. Rebeiz, "Micromachined self-packaged W-Band bandpass filters," in *IEEE MTT-S Symp. Dig.*, 1995, pp. 1543–1546.
[5] J. S. Hong and M. J. Lancaster, "Couplings of microstrip square open-loop resonators for cross-coupled planar microwave filters," *IEEE Trans. Microwave Theory Tech.*, vol. 44, pp. 2099–2109, Dec. 1996.
[6] S. B. Cohn, "Direct coupled resonator filters," *Proc. IRE*, Feb. 1957, pp. 187–196.
[7] G. Matthaei, L. Young, and E. M. T. Jones, *Microwave Filters, Impedance Matching Networks and Coupling Structures*. Dedham, MA: Artech House, 1980.
[8] A. E. Atia and A. E. Williams, "Narrow bandpass waveguide filters," *IEEE Trans. Microwave Theory Tech.*, vol. 20, pp. 258–265, Apr. 1972.
[9] K. Zaki *et al.*, "Narrow bandpass waveguide filters," *IEEE Trans. Microwave Theory Tech.*, vol. MTT-20, pp. 258–265, Apr. 1972.
[10] M. Aubourg and P. Guillon, "A mixed finite element formulation for microwave devices problems. Application to MIS structure," *J. Electromagn. Waves Applicat.*, vol. 5, no. 45, pp. 371–386, 1991.
[11] S. Kim, E. Tuncer, B.-T. Lee, and D. P. Neikirk. (1997). *Surface impedance method for interconnect analysis* [Online]. Available: URL: http://weewave.mer. utexas.edu/MedHome.html.
[12] R. B. Marks, "A multiline method of network analyzer calibration," *IEEE Trans. Microwave Theory Tech.*, vol. 39, pp. 1205–1215, July 1991.
[13] R. B. Marks and D. F. Williams, Multical v 1.00, NIST, Aug. 1995.
[14] R. Levy, "Filters with single transmission zeros at real or imaginary frequencies," *IEEE Trans. Microwave Theory Tech.*, vol. MTT-24, pp. 172–181, Apr. 1976.
[15] R. M. Kurzrok, "General four resonator filters at microwave frequencies," *IEEE Trans. Microwave Theory Tech.*, vol. MTT-14, pp. 295–296, June 1966.
[16] K. Jokela, "Narrow-band stripline or microstrip filters with transmission zeros at real or imaginary frequencies," *IEEE Trans. Microwave Theory Tech.*, vol. MTT-28, pp. 452–460, June 1980.

Pierre Blondy received the Doctorat degree from the University of Limoges, France, in 1998. During his thesis, he studied Micromachined structures and their applications to filters at the University of Limoges and at the University of Michigan, Ann Arbor.

He is currently research engineer at the Centre National de la Recherche Scientifique (CNRS), and he works at the IRCOM Laboratory in Limoges, France. His main field of interest is micromachined devices for millimeter-wave communication systems.

Andrew R. Brown (S'96) received the B.S.E.E. and M.S.E.E. degrees from the University of Michigan, Ann Arbor, in 1995 and 1996, respectively, and is currently working toward the Ph.D. degree in electrical engineering at the same university.

His present research involves applying micromachining techniques to achieve very low-loss transmission lines and high-Q resonant structures for millimeter-wave communication systems.

Dominique Cros received the Doctorat degree from the University of Limoges, France, in 1990.

Currently, he is an Assistant Professor at the University of Limoges working at the Microwave and Optical Communication Research Institute. His main field of interest is millimeter wavelength devices using planar circuits or dielectric resonators.

Gabriel M. Rebeiz (S'86–M'88–SM93–F'97) received the Ph.D. degree in electrical engineering from the California Institute of Technology, Pasadena, in June 1988.

He joined the faculty of the University of Michigan in September 1988 and was promoted to Full Professor in May 1998. He has held short visiting professorships at Chalmers University of Technology, Gothenburg, Sweden, Ecole Normale Supérieure, Paris, France, and Tohoku University, Sendai, Japan. His research interests are in applying micromachining techniques and MEMS for the development of novel components and subsystems for wireless communication systems. He is also interested in Si–GaAs RFIC design for receiver applications, and in the development of planar antennas and microwave/millimeter-wave front-end electronics for applications in mm-wave communication systems, automotive collision-avoidance sensors, monopulse tracking systems and phased arrays.

Professor G. Rebeiz received the National Science Foundation Presidential Young Investigator Award in April 1991 and the URSI International Isaac Koga Gold Medal Award for Outstanding International Research in August 1993. He also received the Research Excellence Award in April 1995 from the University of Michigan. Together with his students, he is the winner of best student paper awards at IEEE-MTT (98-94, 92), and IEEE-AP (95, 92) and received the JINA'90 best paper award. He received the EECS Department Teaching Award in October 1997 and was selected by the students as the 1997–1998 Eta Kappa Nu EECS Professor of the Year. In June 1998, he received the Amoco Foundation Teaching Award, given yearly to one (or two) faculty at the University of Michigan, for excellence in undergraduate teaching.